

A 12-Electrode ECT Sensor with Radial Screen for Fluid Diagnosis

Sidi M. A. Ghaly

Electrical Engineering Department, Imam Mohammad Ibn Saud Islamic University, Saudi Arabia | Ecole Normale Supérieure, Mauritania
smghaly@imamu.edu.sa

Mohammed Shalaby

Electrical Engineering Department, Imam Mohammad Ibn Saud Islamic University, Saudi Arabia
myshalaby@imamu.edu.sa

Mohammad Obaidullah Khan

Electrical Engineering Department, Imam Mohammad Ibn Saud Islamic University, Saudi Arabia
okkhan@imamu.edu.sa

Khaled A. Al-Snaie

Electrical Engineering Department, Imam Mohammad Ibn Saud Islamic University, Saudi Arabia
kalsnaie@imamu.edu.sa

Asad Ali Mohammed

Electrical Engineering Department, Imam Mohammad Ibn Saud Islamic University, Saudi Arabia
asad207@imamu.edu.sa

Faisal Baloshi

Electrical Engineering Department, Imam Mohammad Ibn Saud Islamic University, Saudi Arabia
fambaluchi@sm.imamu.edu.sa

Abdalmajid Imad

Electrical Engineering Department, Imam Mohammad Ibn Saud Islamic University, Saudi Arabia
aimlathkani@sm.imamu.edu.sa

Majdi Oraiqat

Electrical Engineering Department, Imam Mohammad Ibn Saud Islamic University, Saudi Arabia
mtoraiqat@imamu.edu.sa

Received: 9 May 2023 | Revised: 24 May 2023 and 27 May 2023 | Accepted: 29 May 2023

Licensed under a CC-BY 4.0 license | Copyright (c) by the authors | DOI: <https://doi.org/10.48084/etasr.6030>

ABSTRACT

In this paper, the use of radial screens in an Electrical Capacitance Tomography (ECT) sensor is investigated with the aim of resulting in higher-resolution images. The effect of the screens on the quality of the reconstructed images was simulated. 12-electrode ECT sensors with and without screens were designed and tested. The capacitance between different electrode pairs was measured for two permittivity distributions. The obtained capacitance data were used to reconstruct images using the Projected Landweber Iteration algorithm based on linear and semi-linear ECT models. The sensitivity of the measurements and the accuracy of the obtained images for the ECT sensors with and without screens were analyzed. The main conclusion is that a little improvement in the quality of images can be achieved with the use of 12-Electrode ECT sensors with radial screen.

Keywords-ECT sensor; radial screen; permittivity; fluid dynamics; imaging sensitivity measurement

I. INTRODUCTION

There are many two-phase flow systems in the fields of electrical power generation industry, petroleum industry, chemical industry, and metallurgy industry. In the present time, the two-phase flow pattern recognition is mainly employed as a measuring tool for the flow pattern change criterion or the flow chart to diagnose the flow mode with flow parameters. However, due to the complex nature of the flow mechanism, the use of conventional detection techniques cannot match the large variety of the flow conditions. Electrical Capacitance Tomography (ECT) is a tomography technique developed for the industrial multiphase flow measurement systems. Different materials have different dielectric constants, which are used as a basic principle to calculate the spatial distribution of the dielectric constant inside a flow channel and to figure out the distribution of the working medium in the sensing zone by measuring the capacitance values between the electrodes fixed on the insulating surface of the channel [1-3]. Besides, ECT is a non-invasive technique, exhibiting features such as faster response, economical, being non-radioactive, so it is becoming an indispensable analysis tool in multiphase flow industry. With the increased popularity of ECT, one of the areas that need improvement is the relatively low spatial resolution and this is more pronounced on the pixels further away from the electrodes. This issue is closely related to the soft-field nature of the electric field.

When an image is reconstructed, most algorithms use a matrix called sensitivity map in the inverse process, or in both the forward and inverse steps for an iterative algorithm, such as the well-known Landweber method [4-5]. Recently, a pre-iteration scheme was developed that iteratively updates the sensitivity maps instead of the image, and then uses the final sensitivity map in real time ECT measurement [6]. This method offers fast image reconstruction speed while maintaining the same image quality as the Landweber algorithm does. In practice, the sensitivity maps are produced as the product of the inner electrode fields that are usually calculated by solving the Poisson equations for electric fields. The soft-field nature can therefore be inherited during the construction of the sensitivity map. Further, as the strength of the electrical field reduces, for the locations away from the electrodes, the sensitivity decreases correspondingly. To address such a weakness, different models have been proposed, such as the expanded sensitivity map [7], in which the sensitivity map elements can be produced based on a set of blocks of different sizes. The stability and quality of an image can be improved with the help of typical designed extended sensitivity maps. Also, there are other recommendations on the proper distribution of the image elements in the measurement domain, such as those proposed in [8], where a hierarchical mesh algorithm was demonstrated for ECT image reconstruction by locating progressively the boundaries by refining the mesh. At each step of the hierarchy the image was obtained using the Gauss–Newton (GN) algorithm or the Hierarchical Mesh Regularized Constrained Gauss–Newton (HM-RCGN) algorithm. These algorithms have two advantages: the speed of image reconstruction is significantly

accelerated and the spatial resolution of the reconstructed images is enhanced.

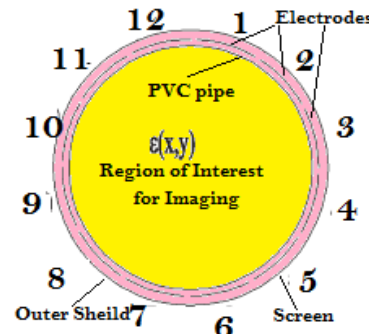


Fig. 1. Cross sectional view of a typical 12-electrode ECT system.

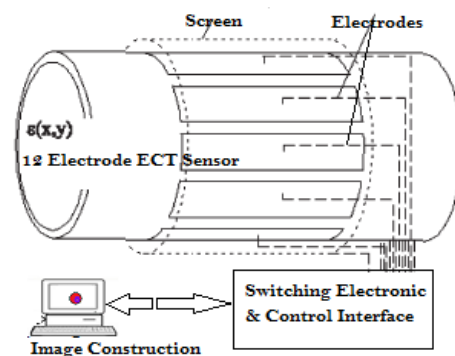


Fig. 2. A typical ECT system with 12 electrodes.

For ECT sensors, the capacitance values are typically small, which requires mounting an earthed screen around the electrodes to eliminate problems related to parasitic capacitance variations that can affect the measurement. Also, the mechanical stability is an important factor in the ECT system. The electrodes are connected to the capacitance measurement system by coaxial connection cables. Thus, in this paper, a 12-electrode ECT sensor with radial screen for diagnosis of fluids was designed and tested. It was shown that it gives better performance in terms of image quality than the one without a radial screen.

II. ELECTRICAL MODELING OF 12-ELECTRODE SENSOR WITH EARTHED SCREEN

Let us consider an ECT sensor with 12 external electrodes with radial screen as shown in Figure 1. These electrodes can be developed with a flexible printed circuit board to a greater precision in its shape and size. In this case, as demonstrated in Figure 1, a 12-electrode sensor needs 66 independent measurements of electrode pairs as: 1-2, 1-3, ..., 1-12; 2-3, 2-4, ..., 2-12; ..., up to 11-12. The ECT systems directly utilize the "raw" capacitance values captured from the sensor to reconstruct images using recursive or iterative algorithms. One of the commonly used algorithms is the Linear Back-Projection (LBP) algorithm for its simplicity and high data rate for image

reconstruction. An LBP image is reconstructed by superposing the sensor sensitivity distribution maps for all electrode pairs by the corresponding measured changes in the normalized capacitance by properly weighting them. When the electrode 1 is biased with a potential, the charge Q_{1j} is generated on the electrodes $j = 2, \dots, N$, that can be measured. Similarly, $Q_{12}, Q_{13}, \dots, Q_{1,N}$, are repeated. Thereafter, electrode 2 is excited and the rest of the electrodes are grounded with potential 0 and the induced charges $Q_{23}, Q_{24}, \dots, Q_{2,N}$ are measured and tabulated. The measurement procedure is repeated until electrode $N - 1$ is energized or excited. Using the measured values of the charge, the inter-electrode capacitances $C_{ij} = C_{ji}$ (with earthed screen) can be calculated using the definition of the capacitance [9-11]:

$$C_{ij} = Q_{ij} / \Delta V_{ij} \tag{1}$$

where Q_{ij} is the induced charge on the electrode j when the electrode i is energized or excited with a known value of voltage. V_{ij} is the voltage between electrodes i and j ($\Delta V_{ij} = V_i - V_j$).

It is a known factor that the capacitance is dependent on the geometry of the electrode and the earthed screen. This can be determined once the size, screen diameter, and location of the electrodes and the permittivity distribution $\epsilon(x, y)$ is known. A change in the permittivity distribution effects the capacitance measurements and the values of capacitance change accordingly. The excitation switching of the electrodes in a sequence produce a rotating electric field inside the typical ECT sensor. It should be noted that the excitation potential is also time varying with a frequency around 1 MHz. For this surrounding situation and the dimension of the ECT sensor and its screen along with the wavelength involved, the electrostatic field theory yields the potential distribution $\phi(x, y)$ inside the ECT sensor [12-13]. On solving the Poisson's equation, we get:

$$\nabla \epsilon(x, y) \nabla \phi(x, y) = 0 \tag{2}$$

For the boundary conditions applied on the ECT sensor headed by the measurement system, the potential distribution $\phi(x, y)$ can be computed. The electric field vector $\mathbf{E}(x, y)$ and the potential function $\phi(x, y)$ are related to each other by:

$$\mathbf{E}(x, y) = -\nabla \phi(x, y) \tag{3}$$

The charge on each of the electrodes, and the inter-electrode capacitances, can be calculated using the definition of the capacitance and Gauss's law based on the surface integral given by:

$$Q_{ij} = \frac{1}{\Delta V_{ij}} \int_{S_j} \mathbf{D} ds \tag{4}$$

\mathbf{D} is the electric displacement defined by:

$$\mathbf{D} = \epsilon(x, y) \mathbf{E}(x, y) \tag{5}$$

The material inside the ECT sensor has a linear isotropic response [19]. S_j is a surface enclosing electrode j , and ds is an infinitesimal area on it.

To solve the Poisson's equation and to calculate the capacitances using Gauss's law, a forward model is considered which shows well behaved and response. The verifications of this forward model against measurements exhibits that the

predicted capacitances are very accurate. At the same time the permittivity sensitivity as observed in [14], the prediction error may be enlarged for adjacent electrodes, when a high permittivity material is surrounded in their vicinity. More information on the use of Finite Element Modelling (FEM) of ECT systems can be seen in [15-16].

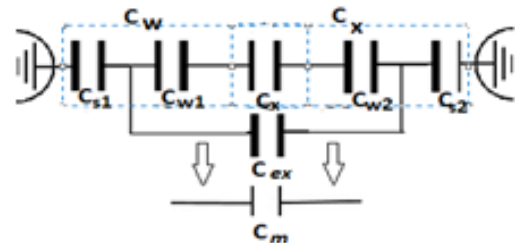


Fig. 3. Electrical modeling.

Consider a model of measured capacitance C_m for one pair of electrodes with the effect of the earthed screen. This can be assumed as the combination of an internal capacitance C_x , two pipe wall capacitances C_{w1}, C_{w2} , an external capacitance C_{ex} , and two stray capacitances C_{s1}, C_{s2} as demonstrated in Figure 3. The equivalent capacitance C_m can be calculated mathematically as:

$$C_m = C_{ex} + \frac{C_w C_x}{C_w + C_x} \tag{6}$$

The values of C_{ex}, C_w , and C_x can be obtained by filling a material of known relative permittivity ϵ_{r1} into the specimen pipe sensor. This procedure is repeated with another material of known relative permittivity ϵ_{r2} and the air. After this, by finding C_{ex} and C_w , the internal capacitance with any fluid existing inside the region of interest in the PVC pipe can be obtained from the raw measured capacitance.

III. SIMULATION OF THE 12-ELECTRODE ECT SENSOR WITH EARTHED SCREENS

The simulation was conducted for a cross-sectional circular view point which can be a cylindrical container made up of insulating material. ECT is difficult to perform on metallic container as the metals leak the electrical charge all over the surface and allow making wrong assumptions. On an insulating frame, the electrodes are fixed, an earthed screen is mounted around them, and a voltage is applied to it when the current passes through the non-metallic cylinder from inside and through the fluid or gas. This makes a small charge to hold in the fluid or gas and creates a capacitance. When one of the electrodes is excited, the other 11 electrodes will act as grounded, and the 12-ECT will be like 11 capacitors along the surface of the cylinder. But since the permittivity and the voltage between the plates are very low and the distance between the electrodes is comparatively big, a very low capacitance could be measured. If the permittivity of the fluid or gas is known and its potential breakdown, an increase in voltage below the breakdown voltage can lead to a better performance of the ECT technique.

The 12-electrode ECT simulation was carried out in MATLAB. The simulation shows that with the existence of the earthed screen, the area of the circumference of the cross-sectional area increases. As the number of electrodes is fixed, there will be a little improvement in the coverage of the region under investigation by means of the area for the number of capacitors used, improving the diagnosis of the flow medium in the pipes in the system [15]. The electric potential between the energized electrode 1 and grounded electrodes 2-12 are shown in Figure 4. Electrode 1 is energized at a low voltage of 0.02 V and the electrode 2 is grounded with some stray charge on it, as the metal electrodes cannot be charged after applying electric field.

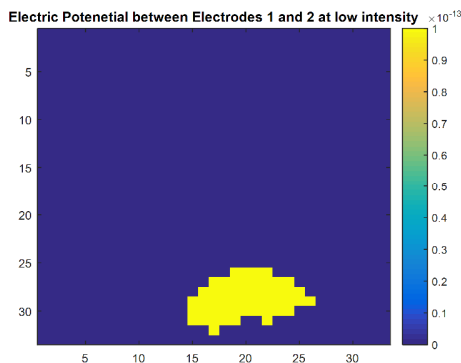


Fig. 4. Sensitivity pattern when electric potential is applied between electrodes 1 and 2 at low intensity.

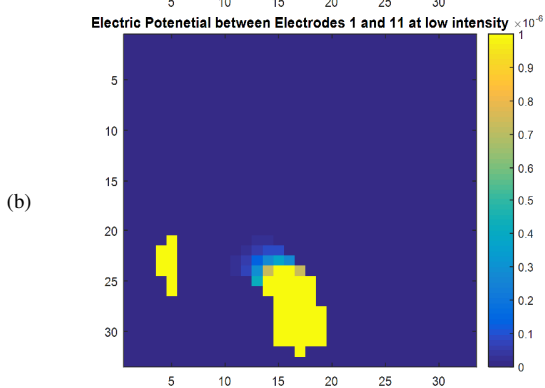
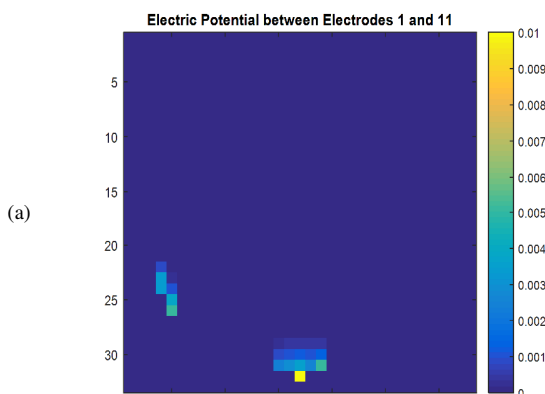


Fig. 5. Sensitivity pattern when the electric potential is applied between electrodes 1 and 11 at (a) normal and (b) low intensity.

Similarly, electrode 1 is energized at a low voltage of 0.02 V and the electrode 11 which has some stray charge on it, is grounded. The electrode potential for 1 and 11 is illustrated in Figure 5. This can be demonstrated for all combinations of 1 to 12 electrodes in the ECT sensor. In the simulation, the first electrode is energized and other electrodes are kept at ground, this process is repeated for all electrodes to be energized one after the other in a cyclic manner, keeping the other electrodes grounded. With increase in the number of electrodes, the circumference of the pipe is more covered and a continuity of measurement is achieved near the inner surface area of the pipe.

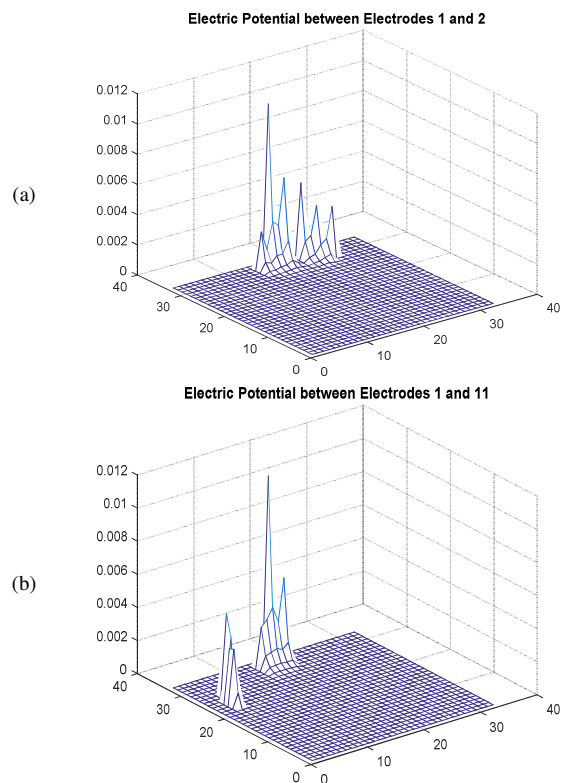


Fig. 6. Sensitivity pattern map of the electric potential between electrodes (a) 1 and 2 and (b) 1 and 11.

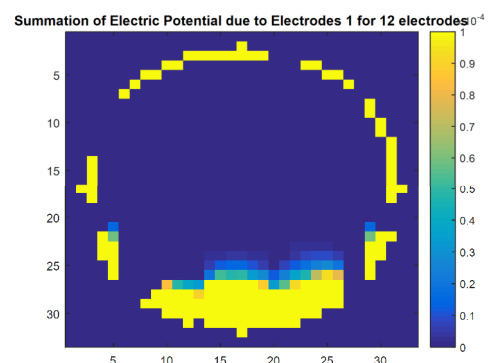


Fig. 7. Summation of the sensitivity pattern due to electrode 1 for all 12 electrodes.

It is evident from the simulations that mounting an earthed screen covers a comparatively large area. It is also seen that the voltage drops very fast as it moves from one end of the diameter to the other, and the increased distance between the electrodes drops the voltage, but for the electrodes which are placed in adjustment to each other there is a good capacitance response. Thus, with an earthed screen, there will be a better accuracy towards the inner side of the pipe near the surface of the pipe compared to the center of the pipe where getting exact accuracy is difficult due to the low voltage measurement and thus the low capacitance measurement. The expected accuracy is more likely to increase with small cross-sectional area pipes compared to that of large cross-sectional area pipes in the system.

IV. IMPLEMENTATION FOR SENSITIVITY MEASUREMENT

The AC-ECT system comprises of hardware and software, software drivers, and ECTGUI. The hardware consists of a front-end unit with an internal power supply, and an NI DAQ board/card interfaced with each other. These are operated by a host laptop or desk top, as illustrated in Figures 2 and 8. Two NI DAQ units are employed: NI PCI-6024E DAQ board working with a desktop PC and NI PCMCIA 6062E DAQ card working with a laptop PC. Both NI DAQ units are connected via a 68-way ribbon cable with the same female connectors in the end connecting to the 19" Euro case, while a different female connector is used in the other end connecting to either the desktop PC or the laptop PC [17].



Fig. 8. Typical 12-electrode ECT sensor setup and ECT system.

The experimental results using the 12-electrode ECT sensor with and without screen are presented in this section. By quantifying the sensitivity, the accuracy of the sensor depends not only on the physical dimensions of the electrodes, but also on the specifications of the earthed screen. If the tube wall is manufactured using dielectric material, the electrodes can be installed inside or outside it, whereas, if the wall is made up of conductive material, the electrodes can be mounted externally. In the present case, the proposed design is employing dielectric materials, hence the electrodes are put outside the pipe and the earthed screen is mounted around them, thereby availing the simplicity of the design. The choice of the number of electrodes and the outer screen depend on the value of the capacitance, the complexity of the circuit, and the data acquisition rate. In case of using more electrodes, the quality of the image would be better at the cost of increased difficulty in measuring capacitances. Commonly, the number of electrodes

used is limited to 8 or 12 (in this article 12 electrodes are considered). A guard electrode is needed to improve the sensitivity measurement and to prevent the electric field from reaching the ground and the end of the measuring electrode. Also, they must be employed if the length of the measuring electrodes is less than twice the sensor diameter approximately. Further, it is essential to add a discharge resistor, in order to avoid the static charge and the damage of a measuring sensor, the resistor should be connected between each electrode and the driven guard and the ground [14]. The typical value of the resistance used is 1 M Ω . A photo shot of the typically developed prototype using 12 electrodes with earthed screen formed from a copper sheet which is bounded around the radial spacers is shown in Figure 8.

The images were obtained using the 12-electrode ECT sensor having relatively long external measurement electrodes (length and width are 15 cm and 1.1 cm). The gap between the electrodes is 0.20 cm. The external circumference and the outer radius of the pipe are 15.6 cm and 2.48 cm. The inner pipe cross section area is 17.84 cm² and the total volume of the ECT section (electrode region) is 17.84 cm² \times 15.6 cm.

A. Sensitivity of the Obtained Image

At first, in order to calibrate the typically designed sensor, two dielectric materials were taken, where the empty state is assumed to be lentils (density of lentils = 46 kg/m³), and the full state is considered as air. Then, different amounts of lentils are introduced into the pipe where the air is surrounding the lentils. A set of measurements are obtained for each case. It can be observed that the smallest volume to be detected has a cross-sectional area of 1.2 cm² (volume = 18 cm³), and mass = 0.83 g).

TABLE I. ECT IMAGES BASED ON DIFFERENT AMOUNTS OF LENTIL FILLING

| | Images based on large amount of lentil | Images based on small amount of lentil |
|---|--|--|
| 12-electrode sensor with radial screen | | |
| 12-electrode sensor without radial screen | | |

A figure of merit is proposed to describe the sensitivity [18] of the 12-electrode ECT sensor with and without a radial screen. A parameter is defined showing the minimum detectable value according to:

$$\text{PoS} = \left[1 - \Delta\epsilon_r \frac{V_{md}}{V_{total}} \right] \times 100 \quad (7)$$

where PoS is the Percentage of Sensitivity, $\Delta\epsilon_r$ is the difference between the dielectric constants of the full and empty state, V_{md} is the minimum detectable volume of the object, and V_{total} is the total volume of the ECT sensor. In the

present case, lentic is the dielectric: $\Delta\epsilon_r = 6$. From the dimensions indicated above, and to calculate the sensitivity, referring to (7), PoS equals to 59.6% with a radial screen and to 50.1% without radial screen. Table I illustrates the obtained images based on different amounts of lentic searching for the minimum detectable volume of the objects (V_{md}).

B. Image Accuracy

In the beginning, the calibration of the sensor was performed to measure its accuracy and authenticity. It is achieved by taking two different dielectric materials with the empty state as air, and the full state as lubricating oil (density = 823 kg/m^3). The amount of lubricating oil introduced in the sensor pipe is such that when the pipe is kept horizontally, it is half filled with the lubricating oil. Figure 9 shows that the separation line between the lubricating oil and the air is deviating from a sharp line. The gradual change from blue color (air) to red color (lubricating oil) is an indication of the accuracy of the sensor with and without earthed screen and their difference. To quantify the accuracy of the ECT sensor, the parameter PoA (Percentage of Accuracy) is proposed as [18]:

$$\text{PoA} = \left(1 - \frac{\text{line thickness}}{\text{image diameter}}\right) \times 100 \quad (8)$$

In the present case and from Figure 9, the PoA is equal to 87%.

Figure 9 illustrates the use of 12-electrode ECT sensors with and without an earthed screen in which line separation between the two different dielectric materials (lubricating oil and air) when the pipe is placed horizontally is demonstrated.

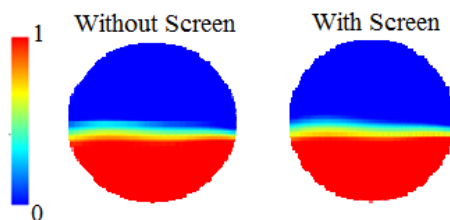


Fig. 9. The line separation between the two different dielectric materials with and without screen.

V. DISCUSSION

In this work, two new parameters, PoS and PoA, were defined with the aim to characterize the quality of an ECT image using an 12-electrode ECT sensor with and without an earthed screen. From the conducted experiments, it is concluded that the use of outer earthed screen gives more accuracy and more sensitivity to the measurements. These conclusions were met while keeping the same gap between the electrodes and for the same cross-sectional area. The Percentage of Accuracy (PoA) with radial screen is found to be equal to 87%, whereas, without radial screen it lies below 84%. The Percentage of Sensitivity (PoS) with a radial screen yields to be 59.6% and 50.1% without a radial screen.

VI. CONCLUSION

In this paper, simulations and practical measurements of an ECT sensor with 12 external electrodes with and without an outer screen were presented. From the simulations, it is evident that a mounted earthed screen covered a comparatively large area. It was also seen that the voltage drops very fast when moving from the one end of the diameter to the other. The experimental measurements were carried out on two different materials filling the space inside the pipe with different proportions in order to know the sensitivity of the measurements and the accuracy of the probe. The obtained images using the 12-electrode ECT sensor with and without an earthed screen, with a line separation between the two different dielectric materials gave a little improvement in the quality of the images produced by developed sensor with a radial screen.

ACKNOWLEDGEMENT

This project was funded by the National Plan for Sciences, Technology and Innovation (MAARIFAH) – King Abdulaziz City for Science and Technology – the Kingdom of Saudi Arabia, award number (14-ELE741-08).

REFERENCES

- [1] K. J. Alme and S. Mylvaganam, "Comparison of Different Measurement Protocols in Electrical Capacitance Tomography Using Simulations," *IEEE Transactions on Instrumentation and Measurement*, vol. 56, no. 6, pp. 2119–2130, Sep. 2007, <https://doi.org/10.1109/TIM.2007.908315>.
- [2] R. Banasiak *et al.*, "Study on two-phase flow regime visualization and identification using 3D electrical capacitance tomography and fuzzy-logic classification," *International Journal of Multiphase Flow*, vol. 58, pp. 1–14, Jan. 2014, <https://doi.org/10.1016/j.ijmultiphaseflow.2013.07.003>.
- [3] D. Chen, Y. Han, J. Huang, L. Wang, and X. Yu, "An Image Data Capture System for Electrical Capacitance Tomography of Oil/Water Two-Phase Flow," in *2006 IEEE International Conference on Information Acquisition*, Weihai, China, Dec. 2006, pp. 722–726, <https://doi.org/10.1109/ICIA.2006.305817>.
- [4] Z. Cui, H. Wang, L. Tang, L. Zhang, X. Chen, and Y. Yan, "A Specific Data Acquisition Scheme for Electrical Tomography," in *2008 IEEE Instrumentation and Measurement Technology Conference*, Victoria, BC, Canada, Feb. 2008, pp. 726–729, <https://doi.org/10.1109/IMTC.2008.4547132>.
- [5] Z. Cui *et al.*, "A review on image reconstruction algorithms for electrical capacitance/resistance tomography," *Sensor Review*, vol. 36, no. 4, pp. 429–445, Jan. 2016, <https://doi.org/10.1108/SR-01-2016-0027>.
- [6] X. Dong and S. Guo, "Modelling an electrical capacitance tomography sensor with internal plate electrode," in *2009 International Conference on Test and Measurement*, Hong Kong, China, Sep. 2009, vol. 2, pp. 160–163, <https://doi.org/10.1109/ICTM.2009.5413087>.
- [7] Z. Fan and R. X. Gao, "A new sensing method for Electrical Capacitance Tomography," in *2010 IEEE Instrumentation & Measurement Technology Conference Proceedings*, Austin, TX, USA, Feb. 2010, pp. 48–53, <https://doi.org/10.1109/IMTC.2010.5488269>.
- [8] S. M. A. Ghaly, "LabVIEW Based Implementation of Resistive Temperature Detector Linearization Techniques," *Engineering, Technology & Applied Science Research*, vol. 9, no. 4, pp. 4530–4533, Aug. 2019, <https://doi.org/10.48084/etasr.2894>.
- [9] Z. Guo, "New normalization method of imaging data for electrical capacitance tomography," in *2011 International Conference on Mechatronic Science, Electric Engineering and Computer (MEC)*, Jilin, China, Dec. 2011, pp. 1126–1130, <https://doi.org/10.1109/MEC.2011.6025665>.
- [10] M. A. Abdelrahman, A. Gupta, and W. A. Deabes, "A feature based solution to Forward Problem in Electrical Capacitance Tomography," in

- Proceedings of the 2010 American Control Conference*, Baltimore, MD, USA, Jun. 2010, pp. 5314–5319, <https://doi.org/10.1109/ACC.2010.5530732>.
- [11] S. M. A. Ghaly, K. A. Al-Snaie, M. O. Khan, M. Y. Shalaby, and M. T. Oraiqt, "Design and Simulation of an 8-Lead Electrical Capacitance Tomographic System for Flow Imaging," *Engineering, Technology & Applied Science Research*, vol. 11, no. 4, pp. 7430–7435, Aug. 2021, <https://doi.org/10.48084/etasr.4122>.
- [12] S. Liu, L. Fu, and W. Q. Yang, "Optimization of an iterative image reconstruction algorithm for electrical capacitance tomography," *Measurement Science and Technology*, vol. 10, no. 7, Apr. 1999, Art. no. L37, <https://doi.org/10.1088/0957-0233/10/7/102>.
- [13] N. Reinecke and D. Mewes, "Recent developments and industrial/research applications of capacitance tomography," *Measurement Science and Technology*, vol. 7, no. 3, Nov. 1996, Art. no. 233, <https://doi.org/10.1088/0957-0233/7/3/004>.
- [14] L. Sheng, S. Yijian, and Z. Guibin, "Design of Data Acquisition System for 12-Electrode Electrical Capacitance Tomography," in *2007 International Conference on Mechatronics and Automation*, Dec. 2007, pp. 2293–2297, <https://doi.org/10.1109/ICMA.2007.4303910>.
- [15] F. Alorifi, S. M. A. Ghaly, M. Y. Shalaby, M. A. Ali, and M. O. Khan, "Analysis and Detection of a Target Gas System Based on TDLAS & LabVIEW," *Engineering, Technology & Applied Science Research*, vol. 9, no. 3, pp. 4196–4199, Jun. 2019, <https://doi.org/10.48084/etasr.2736>.
- [16] Y. Yang, J. Jia, and H. McCann, "A faster measurement strategy of electrical capacitance tomography using less sensing data," in *2015 IEEE International Conference on Imaging Systems and Techniques (IST)*, Macau, China, Sep. 2015, pp. 1–5, <https://doi.org/10.1109/IST.2015.7294533>.
- [17] S. H. Khan and F. Abdullah, "Finite element modelling of electrostatic fields in process tomography capacitive electrode systems for flow response evaluation," *IEEE Transactions on Magnetics*, vol. 29, no. 6, pp. 2437–2440, Aug. 1993, <https://doi.org/10.1109/20.280991>.
- [18] S. Khan and F. Abdullah, "Finite element modelling of multielectrode capacitive systems for flow imaging," *IEE Proceedings Circuits Devices and Systems*, vol. 140, no. 3, pp. 216–222, Jun. 1993, <https://doi.org/10.1049/ip-g-2.1993.0035>.
- [19] P. Kshirgar, "A Robust Noise Reduction Strategy in Magnetic Resonance Images," *Annals of the Romanian Society for Cell Biology*, vol. 25, no. 6, pp. 3938–3952, May 2021.